ELSEVIER

Journal of Photochemistry and Photobiology
A: Chemistry 87 (1995) 89–97

Journal of
PHOTOCHEMISTRY
AND
PHOTOBIOLOGY
A: CHEMISTRY

Time-resolved investigation of radiation trapping for the transition $Sr[5s5p(^3P_1)] \rightarrow Sr[5s^2(^1S_0)] + h\nu$ ($\lambda = 689.3$ nm) following the generation of $Sr[5s5p(^3P_J)]$ by pulsed dye-laser excitation at elevated temperatures

D. Husain *, Jie Lei

The Department of Chemistry, The University of Cambridge, Lensfield Road, Cambridge CB2 1EW, UK

Received 7 September 1994; accepted 11 October 1994

Abstract

We present a kinetic investigation of radiation trapping for the transition $Sr[5s5p(^3P_1)] \rightarrow Sr[5s^2(^1S_0)] + h\nu$ at $\lambda = 689.3$ nm following the pulsed dye-laser generation of $Sr[5s5p(^3P_J)]$ at elevated temperature following excitation of ground state atomic strontium, $Sr[5s^2(^1S_0)]$, at the resonance wavelength. $Sr[5s5p(^3P_J)]$, 1.807 eV above the $^1S_0$ ground state, was produced following laser photolysis to the $^3P_1$ state in a slow flow system, kinetically equivalent to a static system, in the presence of helium buffer gas and at temperatures in the range 670–900 K. Following rapid Boltzmann equilibration within the $Sr(5s5p(^3P_{0,1,2})]$ spin-orbit manifold, time-resolved emission profiles at $\lambda = 689.3$ nm were recorded using signal averaging and computerised analysis techniques under a range of conditions of temperature and pressure, emission from the $^3P_{0,2}$ levels being negligible, these being so-called "reservoir states". First-order decay coefficients ($k'(^3P_J)$) were characterized for the emission at the resonance wavelength as well as integrated atomic fluorescence emission intensities using a sensitivity calibration of the total optical detection system. The resulting mean radiative lifetime for the transition ($\tau_e = 20.7$ μs) was found to be in accord with the results of previous investigations, and the variation of the integrated atomic fluorescence emission intensities with the pressure of helium in accord with considerations of pressure broadening. Furthermore, the absolute second-order rate constant for the quenching of $Sr(5^3P_J)$ by He ($k_Q = (2.9 \pm 0.2) \times 10^{-15}$ cm^3 atoms^{-1} s^{-1} $T = 840$ K) was found to be in accord with the previous upper limit reported for this quantity by time-resolved emission investigations and the value reported from phase-shift techniques. The experimental curve of $k'(^3P_J)$ versus temperature and hence $Sr(5^1S_0)$ density was constructed and compared with the results for radiation trapping according to the theory of (a) Milne, employing the diffusion theory of radiation for low "equivalent opacity" and infinite slab geometry of a thickness comparable with that of the laser beam and (b) Holstein, calculated as a general transport problem by solving a Boltzmann-type integro-differential equation in terms of a transmission coefficient. The results are found to be in accord with the calculations using the theory of Milne. This approach extends the previous empirical corrections that have been made for this effect with $Sr(5^3P_1)$. In more general terms it establishes from fundamentals the importance of radiation trapping for this transition at $\lambda = 689.3$ nm, which, whilst characterised by a relatively large mean radiative lifetime by comparison with that for a fully allowed electric-dipole atomic emission, is, nevertheless, subject to radiation trapping at the densities typically employed with time-resolved measurements following pulsed dye-laser excitation.

Keywords: Ground state atomic strontium; Laser photolysis

1. Introduction

Radiation trapping in atomic emission, namely, the consecutive processes of emission and re-absorption of emitted resonance photons, is a long established physical phenomenon which has been investigated experimentally in terms of the variation of the mean radiative lifetime with the particle density of the lower state, usually the ground state, and in terms of the relationship between fluorescence intensity and particle density in Stern–Volmer measurements [1]. Particular emphasis has been placed on experimental and theoretical considerations of the mean radiative lifetime itself as the basis for investigating fundamentally this phenomenon

* Corresponding author.

SSDI 1010-6030(94)03979-8

including the "escape factor", g, related the effective (τ_{eff}) and natural (τ_e) radiative lifetime ($g=\tau_{eff}/\tau_e$) [2–4]. Clearly, modern electronic methods of data capture are now available for investigating the mean radiative in real time following the optical generation of the excited state. Various theories have been developed to predict this escape factor [2,3,5,6]. Diffusion theories of radiation can essentially be used when the "characteristic mean free path" of a photon, conveniently defined by Deech and Bayliss [7], is significantly greater than the wavelength of the photon itself. For regions of "low equivalent opacities" (Refs. [1,8,9]), Michael and Yeh [8] have demonstrated that the infinite slab diffusion theory of Milne [5], as modified by Samson [10], may be applied from solutions of the appropriate diffusion equation of radiation [5,9], solutions of which have been given in useful form by Blickensderfer et al. [9]. Understandably, extensive attention, for example, has been directed towards radiation trapping in emission from atomic sodium both on account of its fundamental interest, its study in Stern–Volmer fluorescence quenching and, presumably, its use in commercial light sources [4,11–13].

The simplified Samson–Milne–Blickensderfer model will break down at intermediate atomic densities for strongly allowed atomic transitions such as the sodium D-lines when the equivalent opacity becomes reasonably large [14]. One development of this simplified model is that of Kenty [15–18] who employs a Maxwellian distribution in both the absorbing and emitting states. In more general terms, radiation trapping is developed by Holstein [2,3] and modified by Walsh [19] for intermediate to high atomic densities by dispensing with the approximation of the characteristic mean free path of the emitted photon and treating the system as a general transport problem by solving a Boltzmann-type integro-differential equation in terms of a transmission coefficient which is the probability of a photon travelling a given distance without being absorbed. Both the Samson–Milne–Blickensderfer and the Holstein models are explored in this paper to examine radiation trapping for $Sr[5s5p(^3P_1)] \rightarrow Sr[5s^2(^1S_0)] + h\nu$ ($\lambda = 689.3$ nm).

Normally, detailed consideration of radiation trapping is limited to atomic transitions characterised by short mean radiative lifetimes where the absorption cross section of the emitted photon is large and where this effect will be greatest. However, it has already been demonstrated empirically from some reduction in the mean radiative lifetime with temperature and hence ground state atomic density that such an effect is significant in time-resolved measurements on $Sr[5s5p(^3P_1)] \rightarrow Sr[5s^2(^1S_0)] + h\nu$ ($\lambda = 689.3$ nm) [20,21] following pulsed dye-laser excitation. Husain and Schifino [20] have extensively reviewed the earlier literature up to 1984 on the mean radiative lifetime (τ_e) for this transition and, from their time-resolved measurements, report a value of $\tau_e = 20.1$ μs. Subsequently, Husain and Roberts [21] reported $\tau_e = 19.6$ μs and, more recently, Kelley et al. [22] reported $\tau_e = 22$ μs. Whilst such a transition is relatively long-lived, radiation trapping is significant in time-resolved measurements where the $Sr[5s5p(^3P_1)]$ state is generated by pulsed dye-laser excitation at the resonance wavelength from relatively high equilibrium vapour densities of the $Sr[5s^2(^1S_0)]$ ground state which are employed. This may be contrasted with the analogous states of the lighter alkaline earth elements such as $Mg[3s3p(^3P_1)]$ (e.g., $\tau_e = 3.9$ ms [23]) and with comparable earlier values from time-resolved emission methods [24,25]. Chan and Gelbwachs [26] report τ_e for $Ca[4s4p(^3P_1)] \rightarrow Ca[4s^2(^1S_0)] = 408$ μs compared with 331 μs given by Husain and Roberts [27] and 340 μs by Husain and Schifino [28] by time-resolved emission following pulsed dye-laser excitation. Radiation trapping for these longer lived states will clearly be smaller. In this paper, radiation trapping for the transition $Sr[5s5p(^3P_1)] \rightarrow Sr[5s^2(^1S_0)]$ is studied in detail by time-resolved atomic fluorescent emission across the temperature range 670–900 K. The mean radiative lifetime is further examined and found to be in accord with the results of previous time-resolved emission investigations [27,28], and the variation of the integrated atomic fluorescence emission intensities with the pressure of helium in accord with considerations of pressure broadening. The absolute second-order rate constant for the collisional quenching of $Sr(5^3P_J)$ by He has been measured and found to be in accord with the previous upper limit reported for this quantity by time-resolved emission investigations and the value reported from phase-shift techniques. The experimental curve of the first-order rate constant for the decay of $Sr(5^3P_J)$ versus temperature (and hence, density) was constructed and compared with the results for radiation trapping according to the theories of both Milne and Holstein and found to be accord with that of Milne. This approach extends the previous empirical corrections that have been made for this effect with $Sr(5^3P_1)$. In more general terms it establishes from fundamentals the importance of radiation trapping for this transition at the densities typically employed with time-resolved measurements following pulsed dye-laser excitation.

2. Experimental details

The experimental arrangements for monitoring atomic resonance fluorescence, $Sr[5s5p(^3P_1)] \rightarrow Sr[5s^2(^1S_0)] + h\nu$ ($\lambda = 689.3$ nm) in the time-domain were similar to those described in our recent investigations on chemical reactions of $Sr(5^3P_J)$ [29,30] with modifications in analysis for data capture of the time-dependent emission profiles. Thus, $Sr[5s5p(^3P_J)]$ was thus generated, as hitherto, by the Nd:YAG pumped pulsed dye-laser

excitation (10 Hz) (J.K. Lasers, System 2000) of strontium vapour at elevated temperatures [31–33] at $\lambda = 689.3$ nm ($Sr[5s5p(^3P_1)] \leftarrow Sr[5s^2(^1S_0)]$) in the presence of excess helium buffer gas in a slow system, kinetically equivalent to a static system. In contrast to previous methods for data capture of the emission profile [21], the present method employed digitized data capture of complete profiles as opposed to the earlier use of boxcar integration. The decay profiles for $Sr(5^3P_1)$ were recorded using two sets of slits (150 and 600 μm) on the small monochromator (Minichrom, MC1-02, 10288 [29,30]) used for the optimum combination of light gathering power and resolution. The larger slits were normally employed for kinetic measurements: the smaller slits were used to establish the role of slit width and the width of the laser beam, geometrical factors in influencing the boundary conditions of the diffusion equation for radiation. The emission profiles were captured with a "digital storage adapter" (Thurlby DSA 524) interfaced to a computer. 255 decay profiles were captured and averaged as were 255 background profiles before subtraction and transfer for computerised analysis. Measurements of the integrated atomic intensities using the recorded decay profiles required calibration of the response of the optical system. Measurements were made using different photomultiplier voltages for the various atomic profiles. This aspect of the response of the detection system employed the published response characteristic for the gain (G) for the p.m. tube (E.M.I., 9797B, S20 response) which can sensibly be fitted to the form $\ln(G/\text{arb. units}) = 8.7 \ln(V/\text{Volts}) - 54.4$ [34]. Further, the wavelength response of the photomultiplier-grating combination using the Minichrom monochromator was calibrated against a quartz-halogen lamp, one of which had previously been calibrated against a spectral radiometer (International Light Inc., USA. IL783). This yielded two maxima in the sensitivity, one at ca. 440 nm and the other at ca. 510 nm, representing the expected combination of the blaze of the grating for the former and the maximum of photomultiplier tube response (E.M.I. 9797B, S20 response) for the latter [29,30]. All materials (Sr, He) were essentially as employed hitherto [21].

3. Results and discussion

3.1. Intensity and integrated atomic emission profiles

Fig. 1 gives an example of the digitised output indicating the decay of the time-resolved emission $\lambda = 689.3$ nm ($Sr(5s5p(^3P_1)) \rightarrow Sr(5s^2(^1S_0)) + h\nu$) following laser excitation at the resonance wavelength as a function of temperature, and hence density of $Sr(5^1S_0)$, in the presence of excess helium buffer gas. It may be

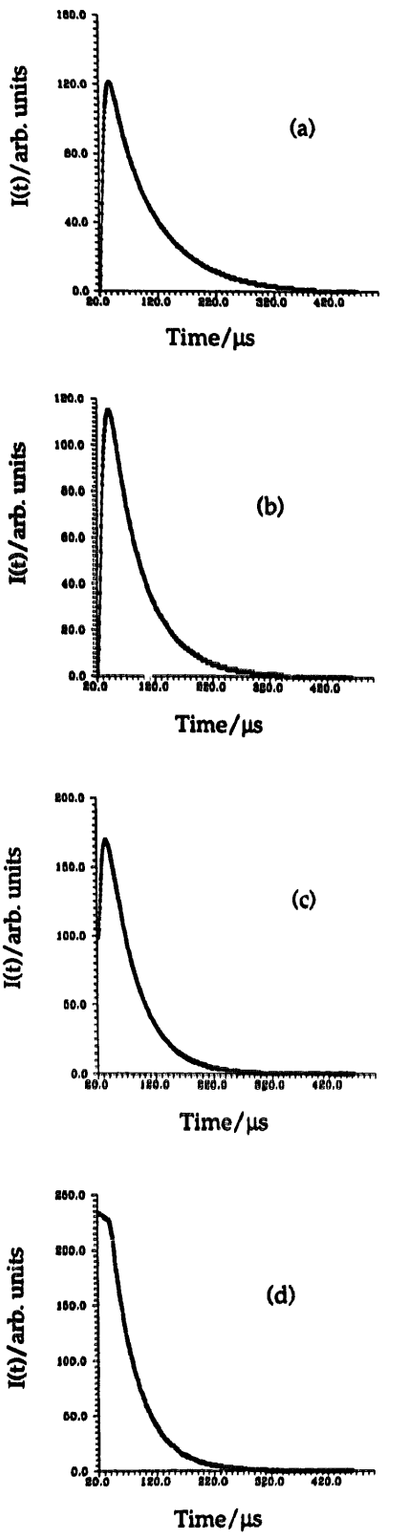

Fig. 1. Examples of the digitised output showing the decay of the time-resolved atomic fluorescence emission, $I(t)$, at $\lambda = 689.3$ nm {$Sr[5s5p(^3P_1) \rightarrow Sr[5s5p(^3P_0)]$} following the pulsed dye-laser excitation of strontium vapour at the resonance wavelength in the presence of helium buffer gas ($p_{He} = 30$ Torr, 3.4×10^{17} atoms cm^{-3}) at elevated temperatures. T(K): (a) 860; (b) 800; (c) 740; (d) 660.

stressed that the gain of the photomultiplier tube is adjusted via the voltage [34] for the lower emission intensity at lower temperatures (e.g., Fig. 1(d) and that the scale is arbitrary. We may see later that this dependence of p.m. gain on voltage (see Section 2) is included in the determination of the integrated atomic emission intensity profiles using the appropriate calibrations. Fig. 2 gives the computerised fitting of the digitised output in Fig. 1 indicating the first-order decay of the time-resolved emission $\lambda = 689.3$ nm $(Sr[5s5p(^3P_1)] \rightarrow Sr[5s^2(^1S_0)] + h\nu)$ after an initial period of ca. 20–50 μs for the decays. One may readily show from approximate calculations of the laser line width and energy output at the resonance wavelength together with estimates of the line shape at $\lambda = 689.3$ nm that it is possible in these measurements to generate densities of $Sr(5^3P_1)$ which are significant compared with those of the $Sr(5^1S_0)$ ground state. This thus yields a kinetic term for the removal of $Sr(5^3P_J)$ involving $[Sr(5^3P_J)]^2$ which is significant and causes departures from linearity in the first-order kinetic plots at earlier times particularly at high laser working voltages. For this reason, the working of the Nd:YAG laser is set in the range 830–850 V. Further, Kelley et al. [35] have characterised the rate constant for self-annihilation between $Sr(5^3P_J)$ which is seen to be large, of the order of the collision number. Thus for this reason, together with the switching of the p.m. gating circuit, there is an initial period before which first-order decay of $Sr(5^3P_J)$ is established. Under these conditions we may then write

$$[Sr(5^3P_J)]_t = [Sr(5^3P_J)]_{t=0} \cdot \exp(-k't) \quad (1)$$

The overall first-order decay coefficient, k', may then be expressed in the form [20,36]:

$$k' = k_{em} + \beta/p_{He} + \Sigma k_Q[Q] \quad (2)$$

where k_{em} represents first-order loss due to radiative decay from $Sr(5^3P_1)$, where the $^3P_0$ and $^3P_2$ states are "reservoir states" from which emission may be neglected [37,38]. The slopes of these first-order plots may then be recast in the form in the standard form [20,36]:

$$k' = A_{nm}/(1 + 1/K_1 + K_2) + \beta/p_{He} + \Sigma k_Q[Q] \quad (3)$$

and thus yield the appropriate decay coefficients in the presence of He alone. K_1 and K_2 represent the equilibrium constants connecting the spin-orbit states within $Sr(5^3P_J)$ ($^3P_0 \rightleftharpoons {}^3P_1$, K_1; $^3P_1 \rightleftharpoons {}^3P_2$, K_2) which rapidly reach Boltzmann equilibrium on the time-scales of the present measurements. Emission is observed only from $Sr(5^3P_1)$ and the term, β/p_{He}, represents diffusional loss of $Sr(5^3P_J)$. The function $F = (1 + 1/K_1 + K_2)$, calculated by statistical thermodynamics, takes the value of 2.307 at $T = 840$ K, for example, and reaches a limiting value of 3 at infinite temperature, being determined solely by statistical weights with $Sr(5^3P_J)$. $\Sigma k_Q[Q]$ represents collisional quenching of $Sr(5^3P_J)$ by He and $Sr(5^1S_0)$.

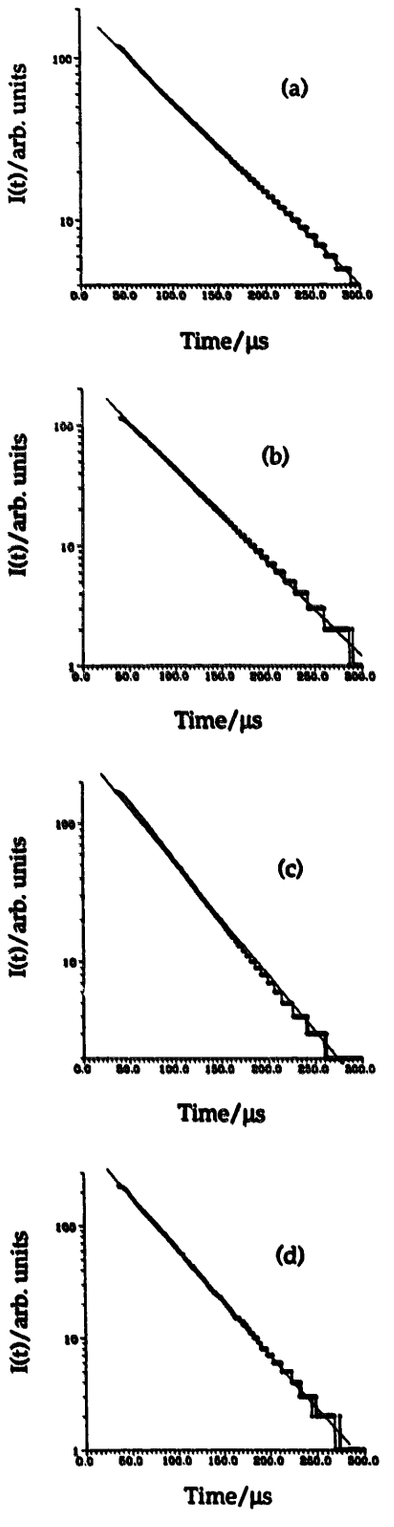

Fig. 2. Examples of the computerised fitting of the digitised output indicating the first-order decay of the time-resolved atomic fluorescence emission, $I(t)$, at $\lambda = 689.3$ nm $\{Sr[5s5p(^3P_1) \rightarrow Sr[5s5p(^3P_0)]\}$ following the pulsed dye-laser excitation of strontium vapour at the resonance wavelength in the presence of helium buffer gas ($p_{He} = 30$ Torr, 3.4×10^{17} atoms cm^{-3}) at elevated temperatures. T(K): (a) 860; (b) 800; (c) 740; (d) 660.

In fact, Eq. (3) must be modified to allow for radiation trapping via the term A_{nm} ($=1/\tau_e$) which is seen to be significant this system. The detailed time scale by which the Boltzmann equilibrium has been reached within the spin-orbit components for $Sr(5^3P_J)$ in helium alone is a matter of some controversy. The application in various publications of such rapid equilibration and the standard use of the 5^3P_0 and 5^3P_2 states as "reservoir states" leads to a mean radiative lifetime of $\tau_e = 19.6^{+0.6}_{-0.5}$ μs [21]. Rapid establishment of this equilibrium is consistent with spectrophotographic measurements made directly on the spin-orbit equilibration on $Ca(4^3P_{0,1,2})$ by McIlrath and Carlsten [39] and, recently, using dye-laser induced fluorescence measurements on the individual spin-orbit states within a 40 ns time scale [40]. Kelley et al. [22], describe time-resolved measurements on the $Sr(5^3P_{0,1,2})$ spin-orbit states using atomic resonance absorption spectroscopic monitoring by means of a hollow cathode source. That work [22] concludes that spin-orbit mixing is a slower process for the heavier noble gases than considered hitherto [22], however, collisionally-induced mixing within $Sr(5^3P_J)$ by He is relatively rapid and the resulting mean radiative lifetime for $Sr(5^3P_1)$ of $\tau_e = 22 \pm 0.5$ μs [22] is not largely different to that reported hitherto and will not significantly affect the present analysis, including the effect of radiation trapping.

Fig. 3 shows the variation of the pseudo first-order rate coefficient, k', for the decay of $Sr(5^3P_J)$ generated by the pulsed dye-laser excitation of strontium vapour at the resonance wavelength ($\lambda = 689.3$ nm, $Sr[5s5p(^3P_1)] \leftarrow Sr[5s^2(^1S_0)]$) at elevated temperature ($T = 840$ K) in the presence of helium gas at different concentrations. This yields a collisional quenching rate constant of $k_Q(Sr(^3P_J) + He,\ T = 840\ K) = (2.9 \pm 0.1) \times 10^{-15}$ cm^3 atoms^{-1} s^{-1} which may be compared with the upper limit of $k_Q \leqslant 2.6 \times 10^{-15}$ cm^3 atoms^{-1} s^{-1} reported by Husain and Roberts [21] by time-resolved emission measurements at $\lambda = 689.3$ nm and the value of $k_Q = 2.57 \times 10^{-15}$ cm^3 atoms^{-1} s^{-1} determined by Malins et al. [41] from phase shift measurements. Care must be taken with the quantitative use of this rate constant as it dependent on the purity of the helium employed. The impurity of the present He is stated as 10 ppm, principally N_2 gas. Collisional quenching of $Sr(5^3P_J)$ by N_2 has been measured by Husain and Schifino [42] as $k_Q(Sr(5^3P_J) + N_2) = (3.2 \pm 0.2) \times 10^{-11}$ cm^3 molecule^{-1} s^{-1} ($T = 950$ K) which is not sufficiently large to account for the observed result. The curvature in Fig. 4 which shows the variation of the integrated atomic emission intensity at $\lambda = 689.3$ nm $\{Sr[5s5p(^3P_1)] \rightarrow Sr[5s^2(^1S_0)]\}$ following the pulsed dye-laser excitation of strontium vapour at the resonance wavelength at elevated temperature ($T = 840$ K) in the presence of helium gas at different pressure using the optical calibrations and electronic calibrations described in the experimental section indicates the role of pressure broadening. The measured intensities, $I(t)_{meas}$, can readily related to the real intensities, $I(t)_{real}$, by the relationship:

$$I(t)_{meas} = G_A G_R S_A S_R I(t)_{real} \quad (4)$$

where G_A is the absolute gain of the photomultiplier tube and at a given working voltage (see Section 2) and G_R is a relative gain, normalised to unity. Similarly, S_A is the absolute optical response of the optical

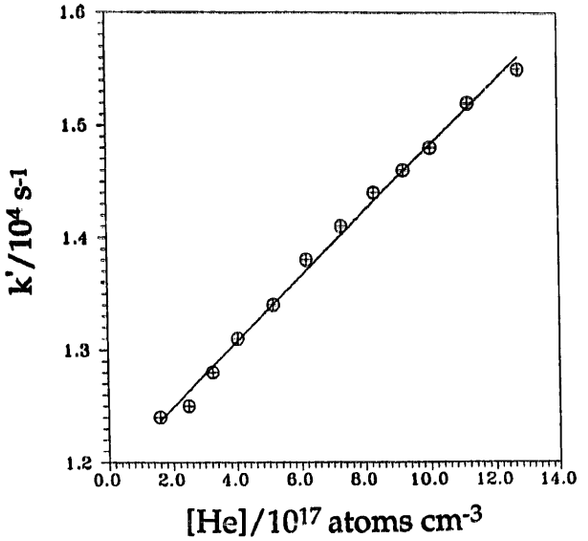

Fig. 3. Variation of the pseudo first-order rate coefficient, k', for the decay of $Sr(5^3P_J)$ generated by the pulsed dye-laser excitation of strontium vapour at the resonance wavelength ($\lambda = 689.3$ nm, $Sr[5s5p(^3P_1)] \leftarrow Sr[5s5p(^3P_0)]$) at elevated temperature ($T = 840$ K) in the presence of helium gas at different concentrations.

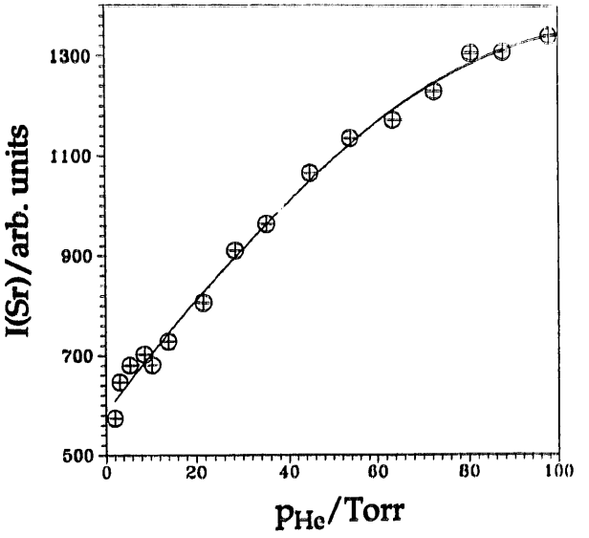

Fig. 4. Variation of the integrated atomic emission intensity at $\lambda = 689.3$ nm $\{Sr[5s5p(^3P_1)] \rightarrow Sr[5s^2S_0)]\}$ following the pulsed dye-laser excitation of strontium vapour at the resonance wavelength at elevated temperature ($T = 840$ K) in the presence of helium gas at different pressure. (Nd:YAG Laser Working Voltage = 840 V).

detection system at the peak of the response curve (see Section 2) and S_R, the response normalised to unity. The absolute intensities are not known in the present measurements but the calibrations described enable the relative intensities, and the integrated intensities to be determined. Considerations of the Doppler width for the transition at $\lambda = 689.3$ nm from the foregoing values of τ_e indicate that the atomic line width is ca. 0.03 cm^{-1}. This can be compared with the line width of the laser, 0.1 cm^{-1}, approximately three times that of the line width. Hence, pressure broadening will increase the yield of excitation to $Sr[5s5p(^3P_1)]$ as indicated in Fig. 4. Further, we may readily estimate the optimum working temperature for maximum laser excitation to yield $Sr(5^3P_J)$. Using $\tau_e = 19.6$ μs (see earlier) as a guide, and the average atomic weight from the isotopic constitution [43] of Sr of $m = 87.62$ we may average over the Doppler line profile and, in turn, estimate an average absorption cross section of $\langle\sigma\rangle = 1.46 \times 10^{-14}$ cm^2. This is in sensible accord with Crane et al. [44]. Let us suppose that the laser beam travels ca. 3 cm to the region of excitation for subsequent observation within $Sr(5^1S_0)$ in the vapour phase and that the resulting attenuation satisfies the standard Beer–Lambert law. Further, suppose then that the subsequent excitation with this attenuated beam directed to generate $Sr(5^3P_1)$ in the small region of observation then satisfies the weak light absorption (namely $I_{abs} = I_0 c\sigma l$) where I_0 is the attenuated beam from the laser initially at a higher value than this I_0, maximization of these two effects with respect to the $Sr(5^1S_0)$ concentration, c, then yields $c = 1/\sigma l_1$ ($l_1 = 3$ cm) = ca. 2.2×10^{13} atoms cm^{-3}. This corresponds approximately to the vapour pressure of strontium in the region $T \sim 800$ K and should be close to the optimum vapour pressure for maximum atomic emission intensity in these measurements. Fig. 5 shows the variation of the integrated atomic emission intensity at $\lambda = 689.3$ nm $\{Sr[5s5p(^3P_1)] \rightarrow Sr[5s^2(^1S_0)]\}$ following the pulsed dye-laser excitation of strontium vapour at the resonance wavelength in the presence of helium gas ($p_{He} = 30$ Torr, 3.4×10^{17} atoms cm^{-3}) at different temperatures, yielding a maximum in sensible accord with these approximate considerations.

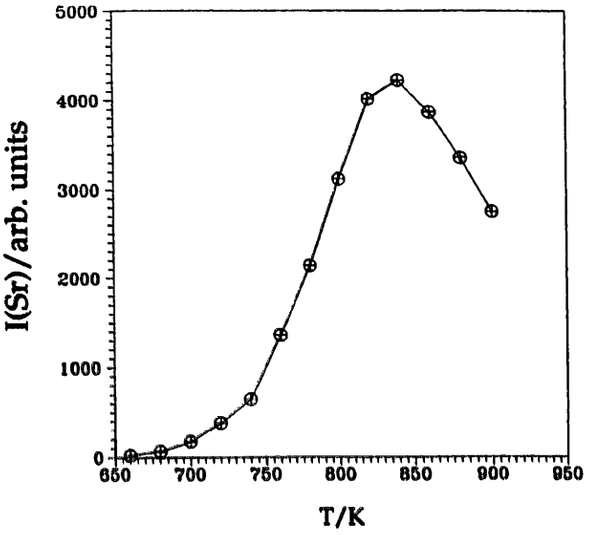

Fig. 5. Variation of the integrated atomic emission intensity at $\lambda = 689.3$ nm $\{Sr[5s5p(^3P_1)] \rightarrow Sr[5s^2S_0)]\}$ following the pulsed dye-laser excitation of strontium vapour at the resonance wavelength in the presence of helium gas ($p_{He} = 30$ Torr, 3.4×10^{17} atoms cm^{-3}) at different temperatures. (Nd:YAG Laser Working Voltage = 830 V).

3.2. Radiation trapping

The present emphasis on radiation trapping is directed towards the "escape factor", $g = \tau_{eff}/\tau_e$ [2–4], as this is dominant effect in this work, rather than the presentation of standard diffusion equations and integrations over line shapes, such as Doppler line shapes for which results will simply be quoted. This escape factor can be incorporated into the measured first-order decay coefficient, k', on the basis of the theory of Milne [5], modifying equation (3), namely,

$$k' = gA_{nm}/F + \beta/p_{He} + k_Q[He] + k_{Sr}[Sr(5^1S_0)] \quad (5)$$

where the symbols have their usual meaning, k_Q and k_{Sr} being the absolute second-order rate constants for the collisional quenching of $Sr(5^3P_J)$. In order to predict the escape factor, various theories have been developed using various simplifying approximations [2,3,5,6]. It is convenient, initially, to consider the theory of Holstein [2,3] who provides a general solution to the radiative diffusion equation in terms of an eigenmode expansion of the following form:

$$n_e(r, t) = \Sigma c_i n_i(r) \exp(-\beta_i t) \quad (6)$$

where $n_e(r, t)$ is the excited atom density at position r and at time t. $n_i(r)$ form a complete set of spacial eigenmodes which is a solution to the diffusion equation corresponding to a pure exponential decay, $\exp(-\beta_i t)$, c_i is the amplitude and β_i the decay rate of the ith mode. The fundamental mode, $i = 1$, is the slowest decaying mode ($\beta_1 < \beta_i, i \neq 1$). In general, the spatial distribution of the excited atom will not decay as a single exponential but will evolve in time towards the fundamental mode distribution, $n_i(r)$, by which time $\beta_1 = 1/\tau_{eff} = 1/g\tau_e$. We may note that, except for the fundamental mode, the spatial modes are non-physical since $n_i(r)$ can be negative for $i \neq 1$. The total excited atom density, $n_e(r, t)$, must, of course, be positive everywhere [12].

Holstein [2,3] has employed the limiting approximation for high optical depth, $k_0 l \gg 1$, where k_0 is the line-centre absorption coefficient and l is a geometric factor. This yields the escape factors of the fundamental mode for Doppler broadening and collision broadening,

respectively, for an infinite slab of thickness, l, [3]:

$$g = = 1.875/\{k_0 l[\pi \log(k_0 l)]^{1/2}\} \quad (7)$$

$$g = 1.150/(\pi k_0 l)^{1/2} \quad (8)$$

Here we will restrict our considerations to the Doppler broadening which is the dominant effect. For the line-centre absorption coefficient of Sr at $\lambda = 689.3$ nm at $T = 850$ K, for example, we may calculate $k_0 = 9.32$ cm^{-1} using the average isotopic mass $m = 87.62$ and neglecting small effects due to nuclear hyperfine structure in ^{87}Sr($I = 9/2$) (6.96%) [43]. Taking the laser beam diameter in these measurements as ca. 0.3 cm, we obtain an optical depth for $T = 850$ K at the wavelength $\lambda = 689.3$ nm of $k_0 l \approx 2.8$. In the working temperature range of these measurements ($T \sim 660$–890 K), on this basis, $k_0 l$ changes from 0.03 to 7.6, essentially in the range for this quantity appropriate for Milne's theory [5]. On this basis, we may thus calculate g for any temperature. An average value for τ_e is taken from literature values [20–22,36,45–47] ($\tau_e = 21 \pm 2$ μs) and the average absorption cross section and absorption coefficient were calculated using the standard expressions for the Einstein coefficients with the average Doppler profile at a given temperature. From previous and past measurements on the decay of Sr(5^3P_J) in He, the diffusion terms $\beta \approx 1500$ Torr^{-1} s^{-1} [20,21], it being recognised that diffusional loss is very small in this system compared with spontaneous emission and, indeed, difficult to detect [20,21]. We employ $k_Q = (2.9 \pm 0.1) \times 10^{-15}$ cm^3 molecule^{-1} s^{-1} following this work (Fig. 3) and $k_{Sr} = 4.7 \times 10^{-14}$ cm^3 atom^{-1} s^{-1} [21]. It must be stressed that the heavily dominant term in equation (5) is the term in gA_{nm}/F.

Fig. 6 shows the comparison of the effects of radiation trapping from the experimental viewpoint expressed in terms of $k'(^3P_J)$ and the temperature, and hence the density of Sr(5^1S_0), and calculations on the basis of the theory of Milne [5] and subsequent modifications (see Section 1). Milne [5] employed a single mean free path for the photons in the vapour ($P(l) = \exp(-\langle k \rangle l)$) and solved the diffusion equation of radiation for an infinite slab of thickness l. This yields the following expression for the fundamental mode escape factor:

$$g = 1/\{1 + (\langle k \rangle l/\lambda_i)^2\} \quad (9)$$

where $\langle k \rangle$ is an average absorption coefficient. λ_i is the first root of the equation

$$\lambda \tan(\lambda) = \langle k \rangle l \quad (10)$$

and varies from $(\langle k \rangle l)^{1/2}$ to $-\pi/2$ as $k_0 l$ varies from 0 to 20 which is the region across which the theory of Milne [5] may be applied. Fig. 6(a) and (b) include experimental data taken with different slit widths (600 and 150 μm) demonstrating that the results are determined by the laser width and not the slit width in terms of the boundary conditions of the diffusion equation. Clearly, emission intensity measurements at $\lambda = 689.3$ nm can be taken at lower temperatures using a wider slit on account of light gathering power but the variation of k' vs. T remains essentially unchanged with slit width. The geometric factor is principally governed by the width of the laser beam. Thus the theory of Milne supports the present results and in accord with previous work on atomic sodium emission

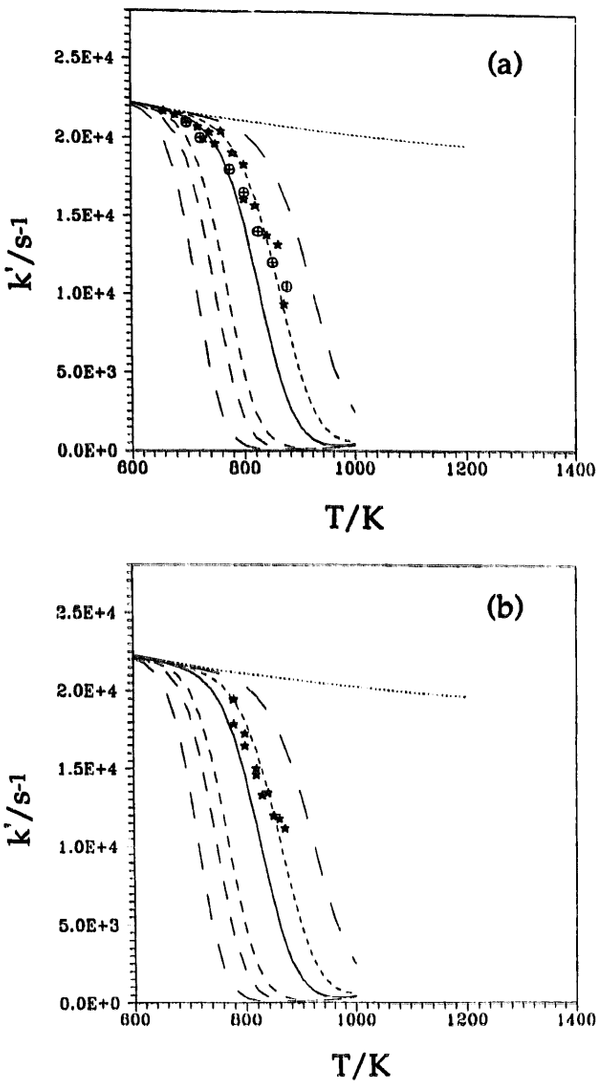

Fig. 6. Results of experimental and theoretical analyses of the effect of radiation trapping on the first-order rate coefficient (k') for the decay of Sr(5^3P_1) $\lambda = 689.3$ nm {Sr[5s5p($^3P_1$) → Sr[5s5p($^3P_0$)]} following the pulsed dye-laser excitation of strontium vapour at the resonance wavelength in the presence of helium buffer gas ($p_{He} = 30$ Torr, 3.4×10^{17} atoms cm^{-3}) at elevated temperatures. Monochromator slit widths (a) 600 μm, (b) 150 μm.

S-shaped curves from right to left corresponding to the calculation of k' according to the diffusion theory of Milne using different thicknesses (l) of the "infinite slab". 1 (cm): 0.03, 0.12, 0.30, 1.50, 3.00, 9.00. Upper dashed line: $k'/s^{-1} = A_{nm}/F$. Stars and crossed circles: experimental data.

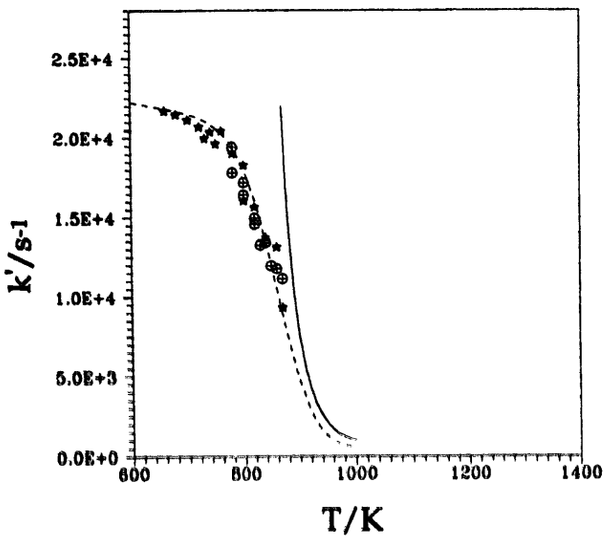

Fig. 7. Results of experimental and theoretical analyses of the effect of radiation trapping on the first-order rate coefficient (k') for the decay of $Sr(5^3P_1)$ $\lambda = 689.3$ nm $\{Sr[5s5p(^3P_1) \rightarrow Sr[5s5p(^3P_0)]\}$ following the pulsed dye-laser excitation of strontium vapour at the resonance wavelength in the presence of helium buffer gas ($p_{He} = 30$ Torr, 3.4×10^{17} atoms cm^{-3}) at elevated temperatures using the radiation trapping theories of Milne (dashed curve) and Holstein (full curve). Geometric factor = 0.12 cm. Stars and crossed circles: experimental data. (Monochromator Slit Widths 600 μm).

at low optical depth [48] as $P(l)$ is then nearly exponential. This becomes a poor approximation at high optical depth where more emission escapes via the optically thin wings of the line and the assumption of a single mean free path for the photon becomes less accurate. The extrapolated value for τ_e for $Sr[5s5p(^3P_1)] \rightarrow Sr[5s^2(^1S^0)] + h\nu$ ($\lambda = 689.3$ nm) of 20.7 μs is in accord with previous measurements [20–22].

Fig. 7 gives a comparison of the application of the Milne [5] and Holstein theories [2,3] where the latter is based on Eqs. (7) and (8) for a defined geometric factor. This is to be expected as the Holstein theory breaks down for low values of $k_0 l$ as seen particularly from Eq. (7) for a Doppler-broadened line and as has been observed hitherto for atomic sodium mutatis mutandis [4,11–13]. Thus, in conclusion, radiation trapping is significant in $Sr(5^3P_1)$ under the conditions of pulsed laser excitation for kinetic studies and the phenomenon is in accord with the diffusion theory of radiation as presented by Milne [5] using a single mean free path of the emitted photon.

Acknowledgements

We thank the Cambridge Overseas Scholarship Trustees for a Research Studentship held by J.L. during the tenure of which this work was carried out. J.L. Also thanks the O.R.S. for an award. We also thank the E.P.S.R.C. of Great Britain for the initial purchase of the laser system. Finally, we are also indebted to Dr. George Jones of the DRA (Fort Halstead) for encouragement and helpful discussions.

References

[1] A.G.C. Mitchell and M.W. Zemansky, *Resonance Radiation and Excited Atoms*, Cambridge University Press, 1971.
[2] T. Holstein, *Phys. Rev., 83* (1942) 1212.
[3] T. Holstein, *Phys. Rev., 83* (1951) 1159.
[4] T. Colbert and J. Huennekens, *Phys. Rev., A41* (1990) 6145.
[5] E.A. Milne, *J. London, Math. Soc., 1* (1926) 40.
[6] H.A. Post, *Phys. Rev., A33* (1986) 203.
[7] J.S. Deech and W.E. Bayliss, *Can. J. Phys., 49* (1971) 90.
[8] J.V. Michael and C. Yeh, *J. Chem. Phys., 53* (1970) 59.
[9] R.P. Blickensderfer, W.H. Breckenridge and J. Simons, *J. Chem. Phys., 80* (1976) 653.
[10] E.W. Samson, *Phys. Rev., 40* (1932) 940.
[11] J. Huennekens and A. Gallagher, *Phys. Rev., A49* (1983) 238.
[12] J. Huennekens, H.J. Park, T. Colbert and S.C. McClain, *Phys. Rev., A35* (1987) 2892.
[13] W.P. Garver, M.R. Pierce and J.J. Leventhal, *J. Chem. Phys., 77* (1982) 1201.
[14] C.F. Bell and D. Husain, *J. Photochem., 26* (1984) 229.
[15] C. Kenty, *Phys. Rev., 31* (1928) 997.
[16] C. Kenty, *Phys. Rev., 42* (1932) 823.
[17] M.W. Zemansky, *Phys. Rev., 29* (1927) 513.
[18] M.W. Zemansky, *Phys. Rev., 42* (1932) 843.
[19] P.J. Walsh, *Phys. Rev., 116* (1959) 511.
[20] D. Husain and J. Schifino, *J. Chem. Soc. Faraday Trans. 2, 80* (1984) 321.
[21] D. Husain and G. Roberts, *Chem. Phys., 127* (1988) 203.
[22] J.F. Kelley, M. Harris and A. Gallagher, *Phys. Rev., A37* (1988) 2354.
[23] F. Beitia, F. Castaño and D. Husain, *J. Chem. Soc. Faraday Trans. 2, 86* (1990) 795.
[24] D. Husain and J. Schifino, *J. Chem. Soc. Faraday Trans. 2, 78* (1982) 2083.
[25] D. Husain and G. Roberts, *J. Chem. Soc. Faraday Trans. 2, 82* (1986) 21.
[26] Y.C. Chan and J.A. Gelbwachs, *Chem. Phys. Lett., 178* (1991) 523.
[27] D. Husain and G. Roberts, *J. Chem. Soc. Faraday Trans. 2, 82* (1986) 1921.
[28] D. Husain and J. Schifino, *J. Chem. Soc. Faraday Trans. 2, 79* (1983) 1265.
[29] M.N. Sanchez Rayo, F. Castaño, M.T. Martinez, J.W. Adams, S.A. Carl, D. Husain and J. Schifino, *J. Chem. Soc. Faraday Trans., 89* (1993) 1645.
[30] F. Castaño, M.N. Sanchez Rayo, R. Pereira, J.W. Adams, D. Husain and J. Schifino, *J. Photochem. Photobiol. A: Chem., 83* (1994) 79.
[31] A.N. Nesmiyanov, *Vapour Pressures of the Elements*, Academic Press, New York, 1963.
[32] C. Smithels, *Metals Reference Handbook*, Butterworth, London, 5th. edn., 1976.
[33] R. Hultgren, P.D. Desai, D.T. Hawkins, M. Gleiser, K.K. Kelley and D.D. Wagman, *Selected Values of Thermodynamic Properties of the Elements*, American Society for Metals, Metals Park, OH, USA, 1973.
[34] E.M.I. Catalogue, *E.M.I. Industrial Publications*, 1979.
[35] J.F. Kelley, M. Harris and A. Gallagher, *Phys. Rev., A38* (1988) 1225.

[36] D. Husain and G. Roberts, *J. Chem. Soc. Faraday Trans. 2, 81* (1985) 1085.
[37] C.H. Corliss and W.R. Bozmann, *Experimental Transition Probabilities for Spectral Lines of Seventy Elements*, Nat. Bur. Stand. (U.S.) Monograph 53, U.S. Government Printing Office, Washington, DC, 1962, pp. 388–389.
[38] J. Reader, C.H. Corliss, W.L. Wiese and G.A. Martin, *Wavelengths and Transition Probabilities for Atoms and Atomic Ions*, Nat. Bur. Stand. (U.S.) Ref. Data Serics NSRDS-NBS-68, U.S. Government Printing Office, Washington, DC, 1980, p. 398.
[39] T.J. McIlrath and J.L. Carlsten, *J. Phys. B., 6* (1973) 697.
[40] F. Beitia, F. Castaño, M.N. Sanchez Rayo and D. Husain, *Chem. Phys., 166* (1992) 275.
[41] R.J. Malins, D.J. Logan and D.J. Bernard, *Chem. Phys. Lett., 83* (1981) 605.
[42] D. Husain and J. Schifino, *J. Chem. Soc. Faraday Trans. 2, 80* (1984) 655.
[43] W. Gordy, W.V. Smith and R.F. Trambarulo, *Microwave Spectroscopy*, Dover, NY, 1953, p. 340.
[44] J.K. Crane, M.J. Shaw and R.W. Presta, *Phys. Rev., 49* (1994) 1667.
[45] M.D. Havey, L.C. Balling and J.J. Wright, *Phys. Rev., A13* (1976) 1265.
[46] E.N. Borisov, N.P. Penkin and F.P. Redko, *Opt. Spectr., 59* (1985) 426.
[47] S.R. Langhoff, C.W. Bauschlicher Jr. and H. Partridge, *Int. J. Quantum. Chem., 18* (1984) 457.
[48] B.P. Kibble, G. Copley and L. Krause, *Phys. Rev., 153* (1967) 9.